# Drying of "Amelie" mango (*Mangifera Indica L.*): Influence of temperature on drying rates and shrinkage curves from 50 to 90°C.

**Alfa Oumar Dissa[*1]; Hélène Desmorieux[2]; Aboubakar Almeck[3], Joseph Bathiebo[1], Jean Koulidiati[1]**

[1] *Laboratoire de Physique et de Chimie de l'Environnement (LPCE), Unité de Formation et de Recherche en Sciences Exactes et Appliquée, Université de Ouagadougou, BP7021, Burkina Faso*
[2] *Laboratoire d'Automatisme et de Génie des Procédés (LAGEP), UCBL1-CNRS UMR 5007-CPE Lyon, Bât.308G,43 bd du 11 Nov.1918 Villeurbanne, Université Claude Bernard Lyon1, Lyon, France*
[3] *IRAD, Garoua, CAMEROUN*

(Reçu le 10/11/2008 – Accepté après corrections le 28/09/2009)

**Summary:** In this study, drying rates and shrinkage curves of Amelie mango are established from 50 to 90 °C and the temperature influence is investigated. Results show that drying rates are greatly influenced by drying air temperature and most of the drying process takes place during the falling drying rate period. From 50 to 90°C, drying kinetics are suitably fitted both by Page and Henderson-Pabis models. Drying rates of Amelie mango can be deduced from drying kinetics simulated by these models. Diffusivities identified in this range of temperature increase with increasing temperature and range from $2.12 \times 10^{-10}$ m²s$^{-1}$ to $4.20 \times 10^{-9}$ m²s$^{-1}$. An Arrhenius type of diffusivity law is established from drying data and the activation energy value is evaluated. The product shrinkage is not influenced by temperature and is best fitted by the linear model. The shrinkage coefficient is evaluated to 1.468.

**Key words**: Amelie mango, shrinkage, drying kinetics, drying rate, diffusivity

# Séchage de la mangue "Amélie" (*Mangifera Indica L.*): Influence de la température sur les courbes de vitesses de séchage et de contraction de 50 à 90°C

**Résumé** : Dans cette étude, les vitesses de séchage et les courbes de contraction de la variété de mangue Amelie sont établis de 50 à 90 °C et l'influence de la température est examinée. Les résultats montrent que les vitesses de séchage sont fortement influencées par la température de l'air séchant et la majeure partie du séchage a eu lieu pendant la période de séchage à vitesse décroissante. De 50 à 90 °C, les courbes de séchage sont convenablement ajustées par les modèles de Page et d'Henderson-Pabis. Les vitesses de séchage de la mangue Amélie peuvent être déduites des cinétiques de séchage simulées par ces modèles. Les diffusivités identifiées dans cette gamme de températures croient avec la température et varient de $2{,}12 \times 10^{-10}$ m²s$^{-1}$ à $4{,}20 \times 10^{-9}$ m²s$^{-1}$. Une loi de diffusivité de type Arrhenius a été établie à partir des données de séchage et une valeur de l'énergie d'activation est évaluée. La contraction du produit n'est pas influencée par la température et est bien corrélées par le modèle linéaire. Le coefficient de contraction est évalué à 1,468.

**Mot clés** : mangue Amélie, contraction, cinétique de séchage, vitesse de séchage, diffusivité

[*] Corresponding author : Alfa Oumar DISSA; E-mail : dissa@lagep.univ-lyon1.fr; alfa_dissa@univ-ouaga.bf

## 1. Introduction

The dried mango represents a great proportion of dried fruit export in West Africa. In the case of Burkina Faso, the seasonal production of mango is about 47600 to 54000 tons and its exports has gone up from 602.1 to 4921.2 tons respectively from 1992 to 2005 [1]. In spite of the increase in these exports, great quantities of harvest (about 50% of the national production) are lost each season because of inadequate means of preservation. Thus, drying could constitute an efficient solution to this problem of conservation. For West African mango fruits, the mode of drying used in industry and traditionally is convective drying and Amelie is the most commonly variety used for drying and exportation. The knowledge of drying rates and the shrinkage behaviour of this variety is then necessary for a better understanding of the drying process and for having dried fruits which respect the standards of external markets. It is in this context that this work was carried out. During these last years, few studies related to the mango drying. Goyal et al. [2] studied the thin-layer drying kinetics of raw mango slices at 55, 60 and 65°C. When studying drying of mango pulp in vacuum, Jaya & Das [3] developed an exponential correlation which allowed determining mango diffusivity as a function of initial thickness and drying medium temperature. Touré et al. [4] studied the free convection sun-drying of cassava, banana and mango and established an expression linking slices initial moisture content to the maximal temperature difference between drying air and each product. Most of these works did not deal with the influence of temperature on the shrinkage behaviour and the drying rates of mango whereas these physical sizes are part of the main parameters which control the drying process of fruits. Therefore, the objective of this study is to investigate that influence of temperature and then to contribute to the setting of the mango drying process.

### Nomenclature

| | |
|---|---|
| $D$ | diffusion coefficient ($m^2s^{-1}$) |
| $d$ | thickness of the sample ($m$) |
| $D_0$ | Arrhenius pre-exponential factor ($m^2s^{-1}$) |
| $E_a$ | activation energy ($Jmol^{-1}$) |
| $L$ | Length of the slab ($m$) |
| $l$ | half thickness of the sample ($m$) |
| $MR$ | moisture ratio |
| $m$ | mass ($kg$) |
| $\dot{Q}$ | drying rate ($kg\ kg^{-1}\ s^{-1}$) |
| $R$ | perfect gas constant, $R$=8.3145 $Jmol^{-1}K^{-1}$ |
| $R^2$ | coefficient of determination |
| $RH$ | relative humidity (%) |
| $RMSE$ | root mean square errors |
| $S$ | surface |
| $S_b$ | bulk shrinkage |
| $T$ | temperature (°C, °K) |
| $t$ | drying time ($s$) |
| $V$ | volume ($m^3$) |
| $V_a$ | air velocity ($ms^{-1}$) |
| $X$ | dry basis moisture content ( $kg_w\, kg_{dm}^{-1}$) |
| $W$ | Width of the sample ($m$) |
| *Greek letters* | |
| $\beta$ | linear shrinkage coefficient |
| $\rho$ | density ($kgm^{-3}$) |
| $\chi$ | reduced chi-square |
| *Subscripts* | |
| $a$ | air |
| $db$ | dry basis |
| $dm$ | dry mass |
| $eff$ | effective |
| $eq$ | equilibrium |
| $exp$ | experimental |
| $m$ | model |
| $o$ | initial |
| $s$ | solid |
| $v$ | vapor |
| $w$ | water |

## 2. Materials and Methods

### 2.1. The mangoes

The Amelie variety used in this study was purchased from a local fruit market of Bobo Dioulasso, town in the west of Burkina Faso. For measures, good quality fruits were selected and washed into water to which a small quantity of Natrium hypochlorite was added as disinfectant, rinsed with drinking water and peeled. The pulp was separated from the stone and sliced through according to the desired thickness.

## 2.2 Maturity measurement

The maturity index of mango fruits was evaluated by the ratio of total soluble solids (in °Brix) and acidity (in mmol/g) as:

$$I_{maturity} = \frac{total\ soluble\ solids\ (°Brix)}{Acidity\ (\frac{mmol}{g})} \quad (1)$$

2.2.1 Total soluble solids

The total soluble solids of mango samples was measured with a hand refractometer Master-α (ATAGO P-1, 0-33°Brix, Japan) initially calibrated with a 20°Brix saccharose solution. For the measures, a few drops of mango juice obtained by pressing a sample were placed in a tissue and put down on the refractometer. The total soluble solids was thus measured and obtained in °Brix.

2.2.2 Acidity

A 0.01 mol/L NaOH (sodium hydroxide) solution added with a 0.05% phenolphthalein solution allowed measuring the sample acidity. Before each measure, the sample was taken from the fruit and ground in a mixer (MOULINEX, 140W, France) to have pulp of mango. Three successive acido-basic titrants were obtained for that pulp. From the sodium hydroxide volume used, the number of moles of total acid in the mass of mango pulp is deduced from the matter quantity preservation equation. The fruit acidity is then defined as the ratio of millimoles of hydronium ion per mass of fresh pulp used in grams.

## 2.3. Drying Kinetics

Drying Kinetics of Amelie mango slices were determined using a laboratory dryer (climatic chamber Votsch Industrietechnik, Germany). The schematic diagram of the dryer is shown in Figure 1. The experiments were carried out using a drying air of 10-30 % relative humidity and 0.8-1.6 $m.s^{-1}$ velocity. These characteristics of drying air were sufficient to reach equilibrium water contents corresponding to water activities lower than 0.6, the typical preservation water activity of dried mango according to several authors [1,21,22]. The samples were dried in a perforated square basket, which had a flow cross-section of 10 cm x 10 cm. They were weighted at regular intervals with a Master Pro SARTORIUS precision balance coupled to the chamber. Mass changes with respect to time were noted at different temperatures (50-90 °C). The dry mass was determined by drying samples at 105°C in an oven-dryer during 24 h [5]. At the end of the 24 h of drying, the measured mass for each sample was the dry mass. For each sample, the water content on dry basis at the different instants of drying was then expressed as:

$$X(kg_w / kg_{dm}) = \frac{m(t) - m_s}{m_s} \quad (2)$$

Deduced drying curves were simulated by the semi-empirical models of Page and Henderson -Pabis.

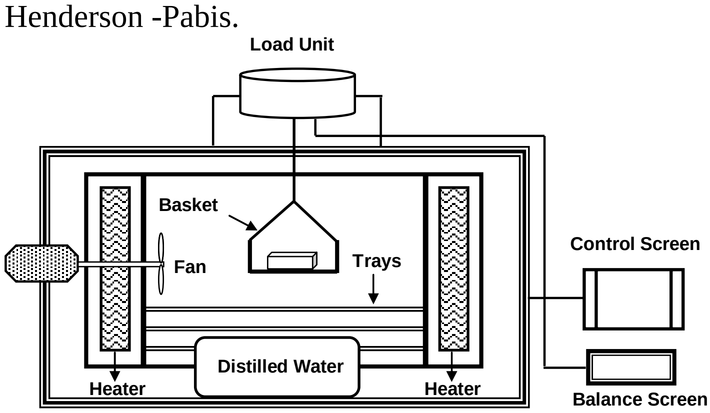


**Figure 1**: Schematic illustration of the experimental dryer set-up.

## 2.4. Bulk shrinkage

Mango slices of parallelepipedic shape were used to establish the mango shrinkage curves. The initial mean dimensions of the samples used during the experiments are presented in Table I. For shrinkage measurements, the product was dried at 50-

90°C in an oven-dryer (WTF BINDER). During drying, the weight of the sample was regularly measured with a balance (SARTORIUS, 0.001g precision, France) every 10 min during the first 110 min. Then, because of the drying rate decrease, measures were taken every 15 min until 300 min drying and then every 30 min until the end of drying, determined by constant weight. During drying, the dimensions of slices were measured using a micrometer ($2x10^{-5}$ m precision). These dimensions were measured at several places of the piece of mango and their mean values were considered. The results of shrinkage measurements obtained are the means of two trials at every temperature. For each measure, the corresponding weights were noted. The bulk shrinkage was then deduced as:

$$S_b = \frac{V}{V_0} \quad (3)$$

Where V is the sample volume at a time t of drying and $V_0$ the initial volume of the sample.
At each instant of drying, V and $V_0$ were calculated as length×width×thickness by assuming that mango slices keep their parallelepipedic shape. The curve of $S_b$ in function of moisture content reported to its initial value is the shrinkage curve. The experimental shrinkage curves obtained were then simulated with a fundamental linear model of volume additivity.

**Table I**: Initial dimensions of samples used for shrinkage measurement

| Temperature (°C) | Length (cm) | Width (cm) | Thickness (cm) |
|---|---|---|---|
| 40 | 5.7 | 4.0 | 1.09 |
| 50 | 5.5 | 3.9 | 1.20 |
| 60 | 5.6 | 4.4 | 1.26 |
| 70 | 6.0 | 3.2 | 1.10 |
| 80 | 6.1 | 3.5 | 1.13 |
| 90 | 6.0 | 3.9 | 1.02 |

## 3. Theory

### 3.1. Drying curves

3.1.1. Simulation

Drying curves were simulated using two empirical models of reduced moisture content: Page and Henderson-Pabis models. These two empirical models coming from the fundamental diffusion model are generally suitable for fruits. The Page model has been successfully used for the drying characteristics description of many products such as carrots, okra and figs [6,7,8], eggplant [9] and fresh and treated Papaya [10]. This model is stated as follow [11]:

$$MR = \frac{X - X_{eq}}{X_0 - X_{eq}} = exp(-kt^{y}) \quad (4)$$

Where: MR is moisture ratio, k and $y$ the parameters of Page model, t the drying time, X the moisture content of the product at the instant t, $X_0$ the initial moisture content and $X_{eq}$ the equilibrium moisture content expressed by Eq. (5) according to [1, 15].

$$X_{eq} = \left[\frac{-ln(1-RH)}{0.0193(T+44.36)}\right]^{1/0.3316} \quad (5)$$

The Henderson-Pabis model is an exponential model obtained by simplification of the first term of the series solution of Fick's second law. It has been used in several works for kiwi fruits [12] and for mulberries [7]. This model effectively predicts the drying rate at the beginning of the drying process but appears sometimes to be less efficient for the last stages of the process. It is expressed as [13]:

$$MR = \frac{X - X_{eq}}{X_0 - X_{eq}} = a\, exp(-bt) \quad (6)$$

Where $a$ and $b$ are the parameters of the Henderson-Pabis model.

3.1.2. Effective water diffusivity determination

The water diffusivity of mangoes is evaluated by using the simplified mathematical Fick's second law. Assuming one-dimensional moisture transfer, homogenous and parallelepipedic shape for the mangoes' samples, uniform initial moisture distribution and a non-shrinking slab, the analytical solution of Fick's equation can be stated as [14]:

$$\frac{X - X_{eq}}{X_0 - X_{eq}} = \frac{8}{\pi^2} \sum_{n=0}^{\infty} \frac{1}{(2n+1)^2} exp\left[ -(2n+1)^2 \frac{\pi^2}{4} \frac{Dt}{l^2} \right] \quad (7)$$

Where $l$ is the half thickness of the slice, $D$ the water diffusivity and $n$ the Fourier's series number.

The water diffusivity is evaluated using slopes method. Its values are determined by plotting experimental drying data in terms of $ln(MR)$ versus $t/l^2$. Activation energy was identified from diffusivity according to Arrhenius dependence as:

$$D = D_0 \, exp\left(\frac{-E_a}{R(T + 273.15)}\right) \quad (8)$$

Where $R$ is the perfect gas constant ($R$=8.3145 $Jmol^{-1}K^{-1}$), $D_0$ the Arrhenius factor ($m^2s^{-1}$), $T$ the temperature (°$C$) and $E_a$ the activation energy for internal mass transfer ($Jmol^{-1}$).

### 3.1.3. Drying rate evaluation

The drying rate was expressed as the mass of water removed per unit of time and per unit of dry mass according to the relation:

$$\dot{Q} = -\frac{dX}{dt} \quad (9)$$

Where $\dot{Q}$ ($kg\, kg^{-1}\, s^{-1}$) is the drying rate and $X$ the water content in dry basis.

The drying rate curves evaluated for each experiment were smoothed using a Microsoft Excel macro-program. This macro initially fitted the series of data by an appropriate polynomial function and then replaced each value of the series by a medium value in such a way that standard deviations from initial values are minimised.

## 3.2. Shrinkage

The bulk shrinkage of foodstuffs during drying is considered by many previous studies[16, 17]. In this work, the influence of temperature on its value is investigated. Experimental shrinkage curves of mango were established at 50-90 °C and simulated using a fundamental linear model. This model is based on the hypothesis of the additivity of volumes of water and solids, assuming that the volume of air in pores is negligible and that cellular tissues are incompressible [18, 19, 20]. If $V$ is the volume of the sample and $m_s$ the dry mass, the volume versus the moisture content on dry basic $X$ is stated as:

$$V = m_s\left(\frac{1}{\rho_s} + \frac{X}{\rho_w}\right) \quad (10)$$

Where: $\rho_s$ is the density of dry mass and $\rho_w$ the density of water.

From Eqs. (3) and (10), the bulk shrinkage can be expressed as:

$$S_b = b' + a'\left(\frac{X}{X_0}\right) \quad (11)$$

With:

$$a' = \frac{\beta X_0}{1 + \beta X_0} \quad (12)$$

$$b' = \frac{1}{1 + \beta X_0} \quad (13)$$

Where $\beta$ is the shrinkage coefficient. The value of $\beta$ was deduced from the ratio of a' and b' as:

$$\beta = \frac{a'}{b'} \times X_0^{-1} \quad (14)$$

This expression gives an estimate of the shrinkage coefficient of mango which is a parameter difficult to determine through direct physical measurements.

## 3.3 Fitting

The different fittings were obtained through a regression program in MATLAB software version 7.0.1. The suitability of each fitting model was evaluated by the values of the coefficient of determination ($R^2$), of the the reduced chi square $\chi^2$ and of the root mean square errors (RMSE). The best fit of the drying parameters (kinetics and shrinkage) were given for $R^2$ values closer to 1, RMSE values closer to 0 and $\chi^2$ values closer to 0.

# 4. Results and discussion

## 4.1 Maturity measurement

Samples maturity was evaluated by °Brix and acidity measurements. These two chemical magnitudes for the whole fruits used were respectively 14.0± *1.7* °Brix and 8.9 ± *3.1* mmol/100$g_{pulp}$. The maturity index represented by the °Brix-acid ratio was estimated at 157.30±54.84 °Brix.g/$mmol_{acid}$ for the whole mangoes used. The rate of dry mass was also evaluated at 13.66 g/100$g_{pulp}$.

**4.2. Influence of temperature on drying rates, drying kinetics and diffusivities**

The influence of temperature on the moisture ratio and drying rate curves was investigated for temperatures ranging from 50 to 90 °C. This influence for a mango slice of 5 mm thick at 50-70 °C is illustrated in Figures 2a, 2b and 3. It can be observed that most of the drying takes place during the falling drying rate period. Also, it can be noticed on Figure 3 that drying rates values strongly increase with temperature. Consequently, the time required to reduce the moisture ratio to any given level in Figure 2 depended on the drying temperature, being highest at 50 °C and lowest at 70 °C. Thus, for a 5 mm thick slice, equilibrium is reached in 250 min at 50 °C, 166 min at 60 °C and 83 min at 70 °C. Fruits and vegetables drying rates increasing with air temperature increasing was reported by many authors for okra [8, 23], for carrot [6], for eggplant [9], for fig [24] and for green bean [25].

The experimental results of drying kinetics were fit using Page and Henderson-Pabis models and the fitting statistics are presented in Table II. The experimental data were well fitted by the two models with similar values of fitting parameters. However, Page's model fitting parameters $R^2$ from 0.9940 to 0.9996 and $\chi^2$ from $4.3428x10^{-5}$ to $4.7429x10^{-4}$ were the highest. As showed in Figure 2, both Page and Henderson-Pabis models suitably describe the experimental drying curves of mango slices and may be assumed to represent Amelie mango drying kinetics profile. Drying rates of Amelie mango (in $kg\ kg^{-1}\ s^{-1}$) can then be deduced from drying kinetics gave by these models (by derivation according to time) as:

For Page model:

$$\dot{Q} = -\frac{dX}{dt} = \alpha_0 t^{y-1}\left(X_0 - X_{eq}\right)exp(-kt^y) \quad (5)$$

For Henderson-Pabis model:

$$\dot{Q} = -\frac{dX}{dt} = \alpha_1\left(X_0 - X_{eq}\right)exp(-bt) \quad (16)$$

With $\alpha_0 = k \times y$ and $\alpha_1 = a \times b$

Where *x*, *y*, *a* and *b* are the parameters of Page and Henderson-Pabis models showed in Table II, $X_0$ the initial water content and $X_{eq}$ the equilibrium water content give by the relation (5).

From the drying curves, were deduced water diffusivities identified from the slopes of $ln[(X-X_{eq})/(X_0-X_{eq})]$ vs. $t/l^2$ fitted straight-line. This linear data fitting was done with a determination coefficient $R^2$=0.9742. Identified diffusivities were presented in Table III, likewise temperature influence on their values were illustrated. These diffusivities range from $2.12x10^{-10}$ $m^2s^{-1}$ at 40 °C to 4.20 $x10^{-9}$ $m^2s^{-1}$ at 90 °C. These diffusivities values can be compared to those obtained by Ruiz-López & García-Alvarado [26] for a Mexican mango variety, which varied from $10^{-10}$ and $2x10^{-9}$ $m^2s^{-1}$. From 40°C to 90°C, diffusivities from Table III and Figure 4 increased with temperature from $10^{-10}$ $m^2s^{-1}$ to $10^{-9}$ $m^2s^{-1}$. Also, $ln(D_{eff})$ decreased almost linearly with the inverse of temperature according to Figure 4. From the slope of the curve $ln(D_{eff})$ *vs.* $1/T$ (Figure 4), the activation energy value was evaluated at 25 kJ/mole. This value was close to 27 kJ/mole, that obtained by Ruiz-López & García-Alvarado [26] for the Mexican variety. From experimental data fitting according to Arrhenius law and for temperature ranging from 40 to 90°C, Amelie mango diffusivity was best expressed by the following equation:

$$D(m^2/s) = 9.625x10^{-6}\ exp\left[\frac{-25000}{R(T+273.15)}\right] \quad (17)$$

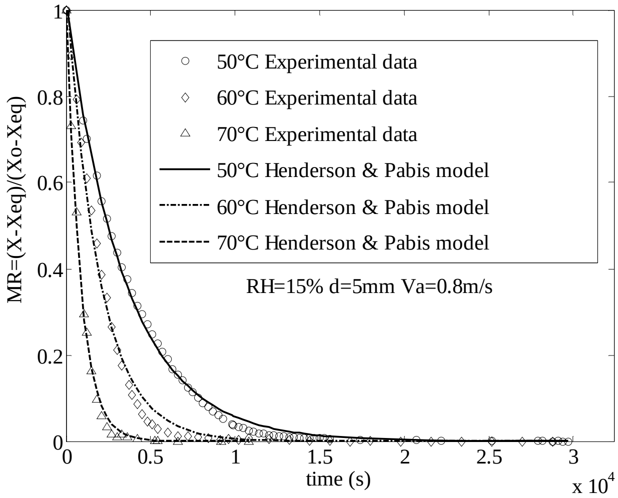


**Figure 2a**: Influence of temperature on the drying kinetics of Amelie mango slices and simulation by Henderson-Pabis model.

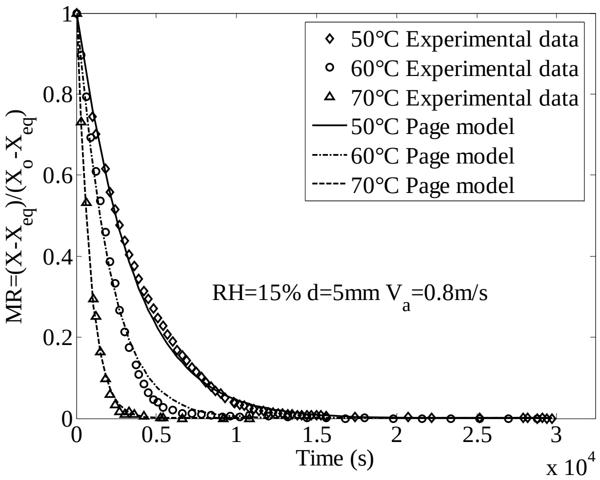


**Figure 2b**: Influence of temperature on the drying kinetics of Amelie mango slice and simulation by Page model.

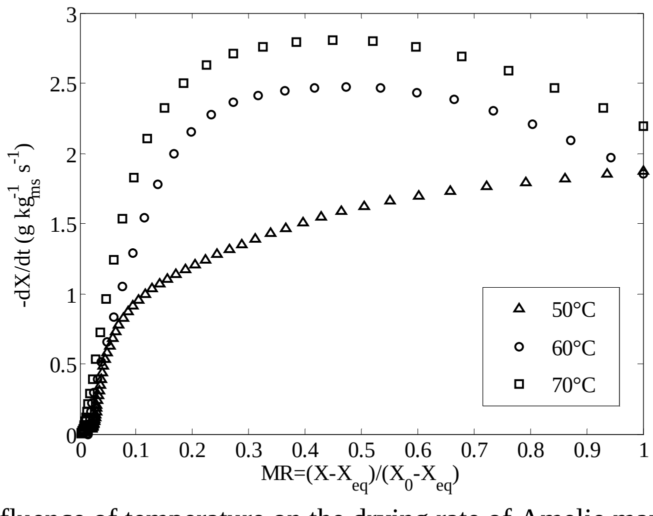


**Figure 3**: Influence of temperature on the drying rate of Amelie mango slice

**Table II**: Fitting statistics of drying kinetics

| Dimensions | | | | | | Henderson-Pabis | | | |
|---|---|---|---|---|---|---|---|---|---|
| L (cm) | W (cm) | d (mm) | $T_a$ (°C) | Va ($ms^{-1}$) | RH % | a | b | R² | χ² |
| 3.6 | 2.6 | 5 | 40 | 1.6 | 30 | 0.965 | $8.872x10^{-4}$ | 0.9934 | $5.6778\ x10^{-4}$ |
| 4.2 | 1 | 5 | 50 | 0.8 | 15 | 1.015 | $2.876x10^{-4}$ | 0.9971 | $1.4957x10^{-4}$ |
| 4 | 1 | 5 | 60 | 0.8 | 15 | 1.060 | $5.167x10^{-4}$ | 0.9923 | $6.1110x10^{-4}$ |
| 3.8 | 0.5 | 5 | 70 | 0.8 | 15 | 1.082 | $4.202x10^{-4}$ | 0.9896 | $1.0x10^{-3}$ |
| 4 | 2.5 | 15 | 80 | 1.6 | 10 | 1.026 | $1.677x10^{-4}$ | 0.9939 | $7.5552x10^{-4}$ |
| 4 | 2 | 10 | 90 | 0.8 | 10 | 1.114 | $2.432x10^{-4}$ | 0.9898 | $1.2x10^{-3}$ |
| | | | | | | Page | | | |
| | | | | | | y | k | R² | χ² |
| 3.6 | 2.6 | 5 | 40 | 1.6 | 30 | 0.943 | $1.651x10^{-4}$ | 0.9909 | $7.8618\ E^{-4}$ |
| 4.2 | 1 | 5 | 50 | 0.8 | 15 | 1.061 | $1.756x10^{-4}$ | 0.9968 | $1.6445x10^{-4}$ |
| 4 | 1 | 5 | 60 | 0.8 | 15 | 1.065 | $2.939x10^{-4}$ | 0.9940 | $4.7429x10^{-4}$ |
| 3.8 | 0.5 | 5 | 70 | 0.8 | 15 | 1.231 | $6.246x10^{-5}$ | 0.9983 | $1.7277x10^{-4}$ |
| 4 | 2.5 | 15 | 80 | 1.6 | 10 | 1.085 | $8.404x10^{-5}$ | 0.9934 | $8.1158\ x10^{-4}$ |
| 4 | 2 | 10 | 90 | 0.8 | 10 | 1.454 | $4.483x10^{-6}$ | 0.9975 | $2.9933\ x10^{-4}$ |

**Table III**: Influence of drying temperature on the water effective diffusivity value

| $T_a$ (°C) | Thickness (mm) | $X_0$ ($kg_{water}kg_{dm}^{-1}$) | $D_{eff}$ ($m^2s^{-1}$) |
|---|---|---|---|
| 40 | 5 | 9.23 | $2.1178x10^{-10}$ |
| 50 | 5 | 8.22 | $7.4951x10^{-10}$ |
| 60 | 5 | 8.59 | $1.6402x10^{-9}$ |
| 70 | 5 | 8.43 | $1.9749x10^{-9}$ |
| 80 | 15 | 9.00 | $3.9602x10^{-9}$ |
| 90 | 10 | 11.86 | $4.1964\ x10^{-9}$ |

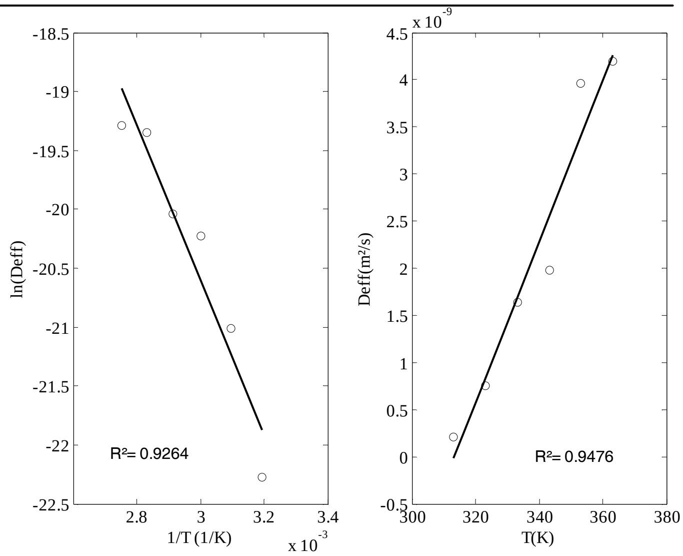


**Figure 4**: Influence of temperature on Amelie mango water diffusivity from 50 to 90°C

### 4.3. Shrinkage

Slices bulk shrinkage coefficient variations with reduced moisture content from 50 to 90 °C are presented in Figure 5. Three samples were used for each temperature and the average shrinkage values were presented. The shrinkage curves obtained were overall linear and almost the same at 50-90 °C. Therefore, it could be deduced that Amelie mangoes shrinkage is not influenced by drying temperatures. The whole of experimental shrinkage curves were linear and could be fitted by the linear model of relation (18). The values of the determination coefficient ($R^2$) and of the root mean square errors (RMSE) are showed in Table IV. These fitting parameters were respectively higher than 0.96 and $1.5863 \times 10^{-4}$ for the range of temperature used. Thus, the linear model of volumes additivity may be assumed to represent the bulk shrinkage of Amelie mangoes at 50-90 °C. This linear model is based on physical assumptions and supposes that the evaporated water volume during drying is replaced by the same volume of shrinkage. The shrinkage coefficient evaluated from the slope of the shrinkage curve was 1.468. This value of the shrinkage coefficient is in accordance with the order of magnitudes given by former similar studies [27] that estimated the density of solid matrix for fruits and vegetables to vary between 1.3 and 1.55.

$$\frac{V}{V_0} = 0.9547 \frac{X}{X_0} + 0.0491 \qquad (18)$$

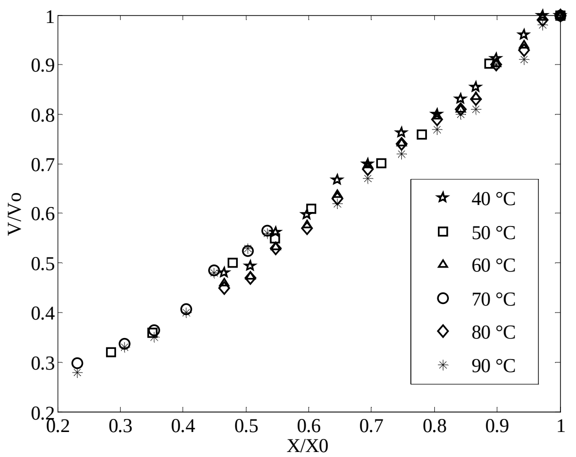


**Figure 5**: Influence of temperature on the bulk shrinkage of Amelie mango slices from 40 to 90°C

**Table IV**: Mango slices shrinkage: experimental data fitting at 50-90 °C with linear additivity model.

| Linear bulk shrinkage coefficients | Ta (°C) | $R^2$ | Standard error |
|---|---|---|---|
| a=0.9547 | **40** | 0.9895 | $1.5863 \times 10^{-4}$ |
| | **50** | 0.9929 | $1.9738 \times 10^{-4}$ |
| b=0.0491 | **60** | 0.9692 | $4.9229 \times 10^{-4}$ |
| | **80** | 0.9937 | $1.3739 \times 10^{-4}$ |
| | **90** | 0.9611 | $6.2704 \times 10^{-4}$ |
| | | 0.9775 | $5.7777 \times 10^{-4}$ |

## 5. Conclusion

In this work, the temperature influence on drying rates and bulk shrinkage of Amelie mango is investigated. Drying kinetics, drying rates and bulk shrinkage were experimentally established and simulated by models at 50-90 °C. It is found that drying rates are greatly influenced by temperature and most of the drying process takes place during the falling drying rate period. Drying kinetics are best fitted both by Page and Henderson Pabis models. Drying rates of Amelie mango can be deduced by differentiation of drying kinetics gave by these models. Effective diffusivities identified at 50-90°C range from $2.12 \times 10^{-10}$ m²s$^{-1}$ to $4.20 \times 10^{-9}$ m²s$^{-1}$. A temperature-dependence law of diffusivity is established from drying data and the activation energy is evaluated. Mango shrinkage curve is not influenced by temperature and is best fitted by the linear model. The shrinkage coefficient deduced from this model is 1.468. This study contributed to the establishment of drying rates curves of mango fruit and to the setting of mango dryer.

***Acknowledgments***

*The authors are grateful to the French Cooperation service in Burkina Faso and the AUF (Agence Universitaire de la Francophonie) for financial support.*

**Bibliography**

[1] Dissa, A., O. Séchage convectif de la mangue: étude de l'influence des paramètres aérauliques et intrinsèques, conception et modélisation du fonctionnement d'un séchoir solaire indirect. Thèse de l'Université de Ouagadougou, Burkina Faso, 27 septembre 2007 ;

[2] Goyal, R.K., Kingsly, A.R.P., Manikantan, M.R., & Ilyas, S.M., Thin-layer Drying Kinetics of Raw Mango Slices. *Biosystems Engineering* (2006) *95 (1)*, 43–49;

[3] Jaya, S., & Das, H., A Vaccum Drying Model of Mango Pulp. *Drying Technology* (2003) *Vol. 21, No. 7,* 1215-1234;

[4] Touré, S., & Kibangu-Nkembo, S., Comparative study of naturel solar drying of cassava, banana and mango. *Renewable Energy* (2004) 29, 975-990;

[5] Nguyen, T., A., Verboven, P., Daudin, J., D., & Bart, M., N., Measurement and modelling of water sorption isotherms of 'Conference' pear flesh tissue in the high humidity range. *Postharvest Biology and Technology* (2004) *Volume 33, Issue 3, 229-241;*

[6] Doymaz, I., Convective air drying characteristics of thin layer carrots. *Journal of Food Engineering* (2004a) *61*, 359–364;

[7] Doymaz, I., Drying kinetics of white mulberry. *Journal of food Engineering* (2004b) *61,* 341-346;

[8] Doymaz, I., Drying charactéristics of okra. *Journal of food Engineering* (2005) *69, 275-279;*

[9] Ertekin, C., & Yaldiz, O., Drying of eggplant and selection of a suitable thin layer drying model. *Journal of food Engineering* (2004) *63,* 349-359;

[10] Anoar, A. E., Patricia, M. A., & Fernanda, E. X. M., Drying Kinetics of Fresh and Osmotically Pre-Treated Papaya. *Journal of Food Engineering* (2003) *59,* 85-91;

[11] Page, G. E. Factors influencing the maximum rates of air drying shelled corn in thin layers. M.S. thesis. Department of Mechanical Engineering, Purdue University, Purdue, USA 1949;

[12] Simal, S. , Femenia, A., Garau, M.C., & Rosselo, C., Use of exponentiel, Page's and diffusional models to simulate the drying kinetics of kiwi fruit. *Journal of Food Engineering* (2005) 66(3), 323-328;

[13] Henderson, S.M., & Pabis, S., Grain drying theory I: Temperature effect on drying coefficient. *Journal of Agriculture Research Engineering* (1961) *6*, 169–174;

[14] Crank, J., The mathematics of diffusion (2nd ed.). Oxford, London: Clarendon Press 1975;

[15] Myara, M. R., & Sablani, S., Unification of fruit water sorption isotherms using Artificial neural networks. *Drying Technology* (2001) *19(8),* 1543-1554;

[16] Suzuki, K., Kubota, K., Hasegawa, T., & Hosaka, H., Shrinkage in the Hydratation of Vegetables Root. *Journal of Food Science* (1976) *41,* 1189-1193;

[17] Lozano, J. E., Rostein, E., & Urbicain M. J., Total porosity and open-pore porosity in the drying of fruits. *Journal of Food Science* (1980) *Vol. 45*(5), 1403–1407;

[18] Desmorieux, H., Le séchage en zone subsaharienne: Une analyse technique à partir des réalités géographiques et humaines. Thèse de l'INPL, France, 1992;

[19] Iglesias, O., Garcia, A. , Roques, M., & Bueno, J. L., Drying of water gels :Determination of the characteristic curve agar-agar. *Drying technology* (1993) *3, 11,* 571-587;

[20] Leonardo, d. S. A., & Dermeval, J.M. S., Dependence analysis of the shrinkage and shape evolution of a gel of system with the force convection drying periods. *In Proceedings of International Drying Symposium (IDS 2004)*, *Sao Paulo, Brazil,* vol.A (pp.152-160), 2004;

[21] Pott, I., Neidhart, S., Mühlbauer, W., & Carle, R., Quality improvement of non-sulphited mango slices by drying at high

temperatures. *Innovative Food Science and Emerging Technologies* (2005) *6, 412-419;*
[22] Desmarais, G., Marcotte, M., Côte d'Ivoire: Coup d'envoi au séchage des mangues et des papayes*.* Canada: CRDA Saint-Hyacinthe, 2002;
[23] Gogus, F., & Maskan, M., Water adsorption and drying characteristics of Okra (*Hibisus Esculentus L.*). *Drying Technology* (1999) *20,* 83-894*;*
[24] Stamatios, J.B., & Vassilios, G.B. Influence of the drying conditions on the drying constants and moisture diffusivity during the thin-layer drying of figs. *Journal of Food Engineering* (2004) *64,* 449-45;
[25] Roselló, C.,Simal, S., SanJuan, N. , & Mulet, A., Nonisotropic mass transfer model for green bean drying. *Journal of Agriculture and Food Chemistry* (1997) *45,* 337-342;

[26] Ruiz-López, I.I., & García-Alvarado, M.A., Analytical solution for food-drying kinetics considering shrinkage and variable diffusivity. *Journal of Food Engineering* (2007) *79,* 208–216;
[27] Lozano, J. E., Rotstein, E., & Urbicain, M. J., Shrinkage, porosity and bulk density of foodstuffs at changing moisture contents. *Journal of Food Science* (1983) *48*, 1497–1502, 1553.